

BRAIN: Bias-Mitigation Continual Learning Approach to Vision-Brain Understanding

Xuan-Bac Nguyen^{1*}, Thanh-Dat Truong¹, Pawan Sinha²,
Khoa Luu¹

¹Dept. of Electrical Engineering and Computer Science, University of Arkansas, AR, US.

²Dept. of Brain & Cognitive Sciences, Massachusetts Institute of Technology, MA, US.

*Corresponding author(s). E-mail(s): xnguyen@uark.edu;
Contributing authors: tt032@uark.edu; psinha@mit.edu;
khoaluu@uark.edu;

Abstract

Memory decay makes it harder for the human brain to recognize visual objects and retain details. Consequently, recorded brain signals become weaker, uncertain, and contain poor visual context over time. This paper presents one of the first vision-learning approaches to address this problem. First, we statistically and experimentally demonstrate the existence of inconsistency in brain signals and its impact on the Vision-Brain Understanding (VBU) model. Our findings show that brain signal representations shift over recording sessions, leading to compounding bias, which poses challenges for model learning and degrades performance. Then, we propose a new Bias-Mitigation Continual Learning (BRAIN) approach to address these limitations. In this approach, the model is trained in a continual learning setup and mitigates the growing bias from each learning step. A new loss function named De-bias Contrastive Learning is also introduced to address the bias problem. In addition, to prevent catastrophic forgetting, where the model loses knowledge from previous sessions, the new Angular-based Forgetting Mitigation approach is introduced to preserve learned knowledge in the model. Finally, the empirical experiments demonstrate that our approach achieves State-of-the-Art (SOTA) performance across various benchmarks, surpassing prior and non-continual learning methods.

Keywords: Continual Learning, Vision Brain Understanding, Neurocomputing, fMRI, Reconstruction

1 Introduction

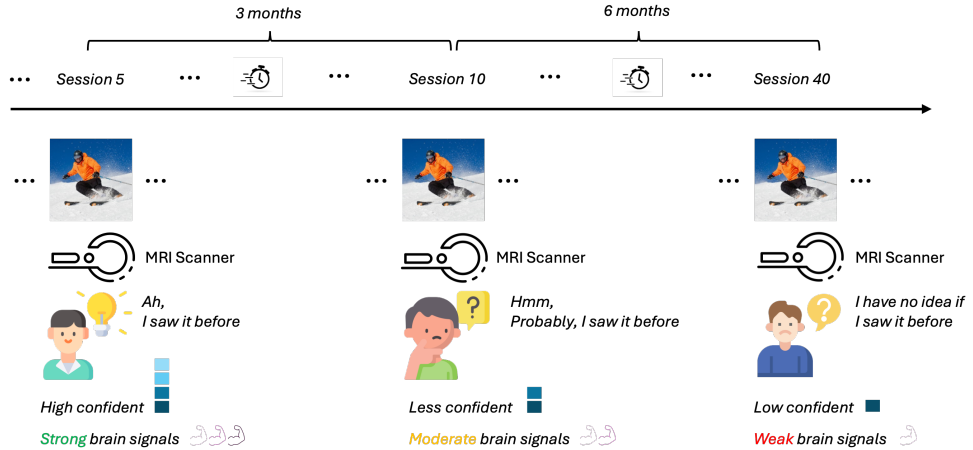


Fig. 1: Participant confidence in recognizing visual stimuli declined over time. Consequently, brain signals from earlier sessions were stronger and contained richer visual context than later sessions. Its shift introduces a distribution change and bias in visual brain signals. While previous studies have overlooked this problem, this work is the first to highlight it.

The human brain is a complex system, with about one-third of its surface dedicated to processing visual information, enabling interpretation, object recognition, and scene understanding [1–4]. Researchers study this process using brain-scanning techniques such as fMRI to gain insights into the connection between vision and brain function [5–10]. Recently, large-scale datasets have been introduced to advance research on vision and brain function [11–13]. Unlike simple collections of instance records, these datasets are built over extended periods, often months or years. For instance, the Natural Scenes Dataset (NSD) took twelve months to complete. During data collection, participants may be exposed to visual stimuli they encountered weeks or months earlier. Prior studies [14–18] on human perception and cognition have shown that the amount of visual information a person can process and retain at any moment is limited by the capacity of visual working memory [19] and varies between individuals. Due to the natural process of *memory decay*, individuals may struggle to recall previously seen stimuli, leading to lower confidence in their responses as demonstrated in Fig. 1. Consequently, fMRI signals recorded in later sessions may exhibit decreased visual contextual information compared to those from earlier sessions.

Limitations in Prior Work. Vision-brain understanding (VBU) has recently made significant strides in decoding brain signals [20–27]. These methods extract visual context hidden within brain signals, often by retrieving or reconstructing the original visual stimuli using generative GANs or Diffusion models. However, they typically treat all data points in the dataset as equal, overlooking the importance of bias in

brain responses [23, 27, 28]. At the same time, they combine all data sessions to train at a time. This limitation can make it challenging for models to learn from fMRI signals recorded in later sessions, where these latter vision brain signals may be more uncertain of visual context and less consistent with earlier data. This problem may lead to a downgrade in the performance of vision-brain models (the details will be provided in Section 3). This paper aims to address the non-stationary problem of brain signals due to the *memory decay* of humans.

Contributions of this Work. Our contributions are summarized as follows¹.

- First, we statistically and experimentally uncover the bias problem in brain signals and its impact on the performance of Vision-Brain models, a problem that most prior studies have overlooked. *To the best of our knowledge, we present one of the first studies to address this bias problem.*
- Second, in a continual VBU setup, brain signals become increasingly inconsistent over time, i.e., across data collection sessions, leading to representation bias in later sessions or training steps. To address this problem, we propose a novel Bias-Mitigation Continual Learning (BRAIN) approach that incrementally learns brain signals throughout the data collection. This approach is designed to mitigate bias and reduce variance in the data.
- Third, we introduce a new *De-bias Contrastive Learning (DCL) loss* to mitigate signal bias and a new *Angular-based Forgetting Mitigation (AFM) loss* to prevent catastrophic forgetting.
- Finally, the empirical results demonstrate the performance improvements of the proposed approach, surpassing previous methods across various continual learning benchmarks.

2 Related Work

2.1 Vision-Brain Understanding

Neural decoding involves interpreting neural signals, e.g., EEG, MEG, fMRI, to infer human perception and cognitive states. Recent advancements have led to substantial progress in this domain, particularly in applications like motor imagery decoding [29] and visual decoding [29–54]. Visual decoding consists of two main tasks: brain-to-image retrieval and reconstruction. Various methods [55–58] have been introduced to align EEG/MEG signal representations with the Contrastive Vision-Language Pre-training (CLIP) [59] embedding space. However, they fail to address the inherent disparities between brain signals and visual stimuli, causing overfitting on the training set and weak generalization to new data. In Vision-Brain Understanding (VBU), fMRI signals recorded while subjects view an image serve as input for reconstructing the initially observed image [22–28]. Several studies have utilized diffusion models [60–64] to model fMRI signal distributions. MindEye [23] employs contrastive learning to align image and fMRI latent spaces before using diffusion models for image reconstruction. MindEye2 [27] adapts to a limited data setting to mitigate the high cost of fMRI data collection. Takagi et al. [22] apply latent diffusion [63] for image

¹The source code of this work will be publicly available.

reconstruction, conditioning on specific fMRI segments. MindBridge [24] introduces a cyclic fMRI reconstruction strategy to align brain data across subjects, facilitating robust brain-to-image and text decoding via dual embeddings. Psychometry [25], in contrast, employs a unified model to extract common and individual features across all subjects. NeuroPictor [26] integrates a latent diffusion-like mechanism [63] to encode fMRI signals into a latent space, distinguishing between high- and low-level features for improved fine-detail focus. UMBRAE [28] employs a vision-language framework to decode fMRI signals, aligning textual descriptions with image features.

2.2 Continual Learning

We review two continual learning strategies [65], each with distinct strengths and limitations. Rehearsal-based methods mitigate catastrophic forgetting by maintaining buffers of past task data [66–105], allowing integration of old and new knowledge to prevent information loss. Some methods employ knowledge distillation to compress information across past and new tasks [68, 70, 71, 75], while others incorporate self-supervised learning techniques [32–36, 38, 40, 42–44, 46–48, 51, 73, 74]. Key challenges include buffer size constraints, excessively small buffers degrade learning [74], and data privacy concerns, which may limit access to stored data [72]. Architecture-based approaches counteract catastrophic forgetting by modifying the model structure. This often involves introducing new parameter sets for each task [106–111] or maintaining specialized sub-networks for different tasks [112–115]. Significant limitations of this method include increased model complexity due to additional parameters and the requirement to identify task types in advance to select the appropriate parameters, not always feasible during inference.

3 Consistency of Brain Signals Analysis

In this section, we analyze the consistency of brain signals across sessions during the collection process. First, we present statistical evidence highlighting inconsistencies in fMRI signals over sessions. Second, we demonstrate the impact of inconsistencies on recent vision-brain decoding models and discuss the importance of addressing this problem.

3.1 Inconsistency in Brain Signals Over Time

From the metadata of NSD, we obtain the response accuracy (Fig. 2 (a) - red line) of participants when determining whether they had seen the current visual stimulus in previous sessions (by pressing a button of Yes or No). Additionally, this data reveals whether participants are consistent with their answers by not changing their minds (Fig. 2 (a) - blue line), with only the final response being recorded. The response accuracy declines over time, while the consistency in their answers also decreases. This pattern suggests growing uncertainty and a lack of confidence among participants as they experience memory decay.

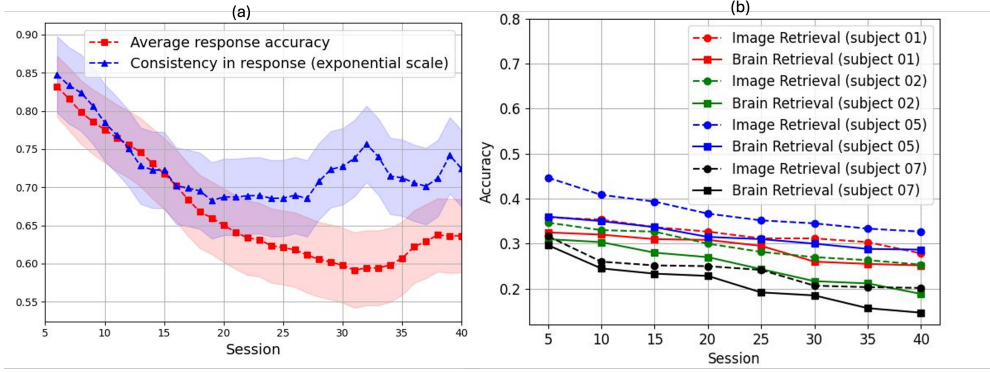


Fig. 2: Data bias due to memory decay. (a) Overall response accuracy (range from 0 - 1) and consistency in their response answers. (b) The retrieval performance of the model was trained every five sessions. **Best view in color**

3.2 Impact of Inconsistency in Brain Signals To Models

To investigate the impact of inconsistency on the brain signals, we utilize a vision-brain retrieval model [27] trained and validated on data from every five sessions. We keep the same model architecture and training parameters across training sessions. The model is evaluated on two tasks: image retrieval, which involves identifying the corresponding image from a given brain signal, and brain retrieval, which involves finding the corresponding brain signal for a given image. As shown in Fig. 2 (b), the results reveal a decline in accuracy across sessions. This trend is likely due to the increasing inconsistency, which diminishes visual context information and makes learning more challenging for the model.

4 The Proposed BRAIN Method

In this section, we will first present our motivation, followed by the problem formulation. Then, we will introduce our proposed De-biased Contrastive Learning and Angular-based Forgetting Mitigation approaches to address the challenges in continual vision-brain understanding.

4.1 Problem Motivation

In Section 3, we have highlighted a key challenge arising from the natural decay of human memory over time. As participants are repeatedly exposed to visual stimuli across multiple sessions, their ability to recognize previously seen images tends to decline in later sessions. This behavioral change introduces a critical issue: ***bias in data representation***, which poses a challenge for models in the Vision-Brain Understanding task. While prior studies have primarily overlooked this problem, addressing it is essential. This paper proposes a novel Continual Learning approach to tackle this issue for several reasons. First, as bias increases over time, i.e., across data collection sessions, a CL approach can adapt to these gradual changes, reducing the risk

of outdated representations. Second, a CL approach aligns with the evolving nature of human memory and perception, making it a more biologically plausible solution than static training paradigms. Lastly, vision-brain data collection spans months or even years. Waiting until all data is collected before training would significantly delay research progress. The CL approach enables incremental model updates after each data collection session, facilitating continuous learning and timely adaptation. In the next section, we will detail the proposed Continual Learning approach to Vision-Brain Understanding.

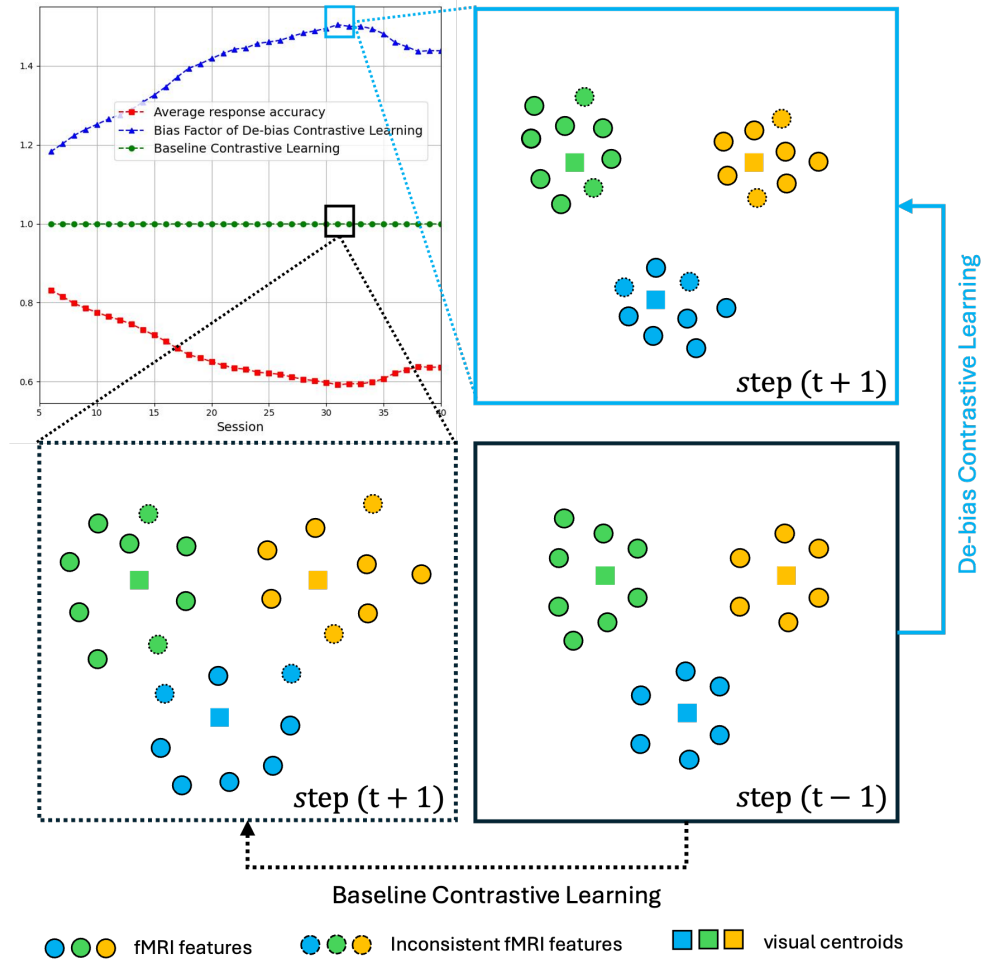


Fig. 3: De-bias Contrastive Clustering.

4.2 Problem Formulation

In continual vision-brain understanding (CVBU), the goal is to learn an fMRI network F on a sequence data $\mathcal{D} = \{\mathcal{D}^1, \dots, \mathcal{D}^T\}$ where T is the number of learning steps. At learning step t , the model F encounters a dataset $\mathcal{D}_t = \{(x^t, y^t)\}$ where $x^t \in \mathbb{R}^n$ is the fMRI signals length of n , and $y^t \in \mathbb{R}^{H \times W \times C}$ is corresponding visual stimuli. Here, we prefer \mathcal{D}_t as the batch of data collected at session t . Let $z^t = F(x^t, \theta_t) \in \mathbb{R}^d$ be the fMRI features, V be a frozen visual encoder that maps visual stimuli y^t to visual centroid $c^t = V(y^t) \in \mathbb{R}^d$, and θ_t is learnable parameters of F . In the CVBU setup, the set of visual centroids \mathcal{C}^t at step t may include both centroids from previous learning steps and newly encountered ones. Formally, the CVBU model at step t can be optimized as Eqn. (1)

$$\theta_t^* = \operatorname{argmin}_{\theta_t} \mathbb{E}_{x^t, y^t \in \mathcal{D}^t} [\mathcal{L}_C(x^t, y^t) + \lambda_{CL} \mathcal{L}_{CL}(x^t)] \quad (1)$$

where the contrastive loss \mathcal{L}_C aligns z^t with c^t , while the continual learning (CL) loss \mathcal{L}_{CL} mitigates forgetting, weighted by the coefficient λ_{CL} . At learning step t , the model F must align fMRI features with previously learned visual centroids and newly encountered visual centroids \mathcal{C}^t . This learning scenario presents two key challenges, i.e., Bias Data Representation and Catastrophic Forgetting. Therefore, we will present our approach to addressing these challenges in the following sections.

4.3 De-bias Contrastive Learning

Limitations in Prior Methods. Since the visual centroid c^t is fixed using the frozen visual encoder V , the contrastive loss term in Eqn. (1) can be rewritten as follows:

$$\mathbb{E}_{x^t, y^t \in \mathcal{D}^t} [\mathcal{L}_C(x^t, y^t)] = \mathbb{E}_{x^t \sim p^t(x)} [\mathcal{L}_C(x^t, y^t)] \quad (2)$$

where $p^t(x)$ represents the distribution of fMRI signals at step t . Prior works [23, 24, 27, 28] have assumed that $p^t(x) = p(x) \quad \forall t \leq T$ and ignored the bias factor. In addition, prior studies [116–118] have suggested that the biased data distribution could negatively influence the contrastive learning, leading to inaccurate representations and resulting in the scatter feature distributions (as shown in Figure 3). To address this problem, we will model the bias factor in the next section and propose a novel loss to mitigate bias in vision-brain signals.

The Proposed De-bias Contrastive Learning (DCL). As demonstrated in Section 3, brain signals have bias in the later sessions, leading $p^t(x) \neq p^{t-1}(x)$. Consequently, Eqn. (2) can be further derived by sampling technique as shown in Eqn. (3).

$$\begin{aligned} \mathbb{E}_{x^t \in p^t(x)} [\mathcal{L}_C(x^t, y^t)] &= \mathbb{E}_{x^t \in p(x)} \left[\mathcal{L}_C(x^t, y^t) \frac{p^t(x)}{p(x)} \right] = \mathbb{E}_{x^t \in p(x)} \left[\mathcal{L}_C(x^t, y^t) \frac{p(x|t)}{p(x)} \right] \\ &= \mathbb{E}_{x^t \in p(x)} \left[\mathcal{L}_C(x^t, y^t) \frac{1}{p(t)} \right] \end{aligned} \quad (3)$$

We call $w^t = \frac{1}{p(t)}$ as a *bias* factor used to measure the difference between $p^t(x)$ and $p(x)$. To efficiently optimize Eqn. (3), we need to model w^t . We observe that

w^t increases over time, indicating a growing bias in data representation. It suggests that $p(t)$ should be a decreasing function over time. Interestingly, in Section 3, the bias increases due to a decreasing in the average response accuracy of participants. Motivated by this observation, we propose a simple yet effective modeling of w^t as follows:

$$w^t = \frac{1}{p(t)} = e^{1-r(t)} \quad (4)$$

where $r(t)$ is the response accuracy at step t . The curve of w^t is illustrated in Fig. 3 (top left). According to this Figure, we infer that a higher weight should be assigned to the loss \mathcal{L}_C at step t if the participant experiences uncertainty or lack of confidence while processing the visual stimuli, and vice versa. The exponential function e helps to maintain the smooth in the bias factor and gradient while optimizing. In summary, we introduce De-bias Contrastive Learning, formulated in Eqn. (5).

$$\mathcal{L}_C(x^t, y^t) = -\log \frac{\exp(z^t \times c^t)}{\sum_{z'} \exp(z' \times c^t)} e^{1-r(t)} \quad (5)$$

4.4 Angular-based Forgetting Mitigation

In continual vision-brain understanding, bias increases in the later learning steps, leading to catastrophic forgetting. Moreover, this bias results in poor and uncertain representations of fMRI signals, making the model susceptible to overfitting to noise and experiencing a significant drop in performance. The forgetting problem is even exaggerated during learning with the gradient descent algorithm, where the model parameters are updated globally. Then, the global changes in the model can significantly influence previously learned knowledge [119].

To prevent the model from forgetting its knowledge learned from previous sessions, prior work has adopted the weight regularization-based approaches [120]. However, these methods remain limited in terms of flexibility and adaptability. Indeed, the regularization-based methods may overly impose updateability of weights, limiting the capability of the model to adapt to new learning data. In addition, the model parameters learned from the previous learning data may not always generalize and adapt well to distribution shifts in the current learning task due to the restrictive update constraints of the weight regularization.

Another approach to prevent catastrophic forgetting in continual learning is distillation, where the model maintains its knowledge by imposing a constraint between predictions of the old and new models [119, 121]. Different from regulation-based methods [120], this approach finds a balance between being adaptable, where the model is enforced to maintain its old knowledge while allowing it to learn new data progressively, and being flexible, which allows the model to continuously update without forgetting. Therefore, in our approach, we propose to model the catastrophic forgetting problem via knowledge distillation. Formally, our continual learning loss, \mathcal{L}_{CL} , in Eqn. (1), can be reformed as:

$$\mathcal{L}_{CL}(x^t) = \mathcal{L}_{CL}(x^t, F, \theta_t, \theta_{t-1}) = \frac{1}{L} \sum_{i=1}^L \mathcal{D}_f \left(F_i(x^t, \theta_{t-1}), F_i(x^t, \theta) \right) = \frac{1}{L} \sum_{i=1}^L \mathcal{D}_f \left(z_i^{t-1}, z_i^t \right) \quad (6)$$

where L is the number of intermediate features, $z_i^{t-1} = F_i(x^t, \theta_{t-1})$ and $z_i^t = F_i(x^t, \theta_t)$ are the i^{th} intermediate feature extracted from model F with θ_{t-1} and θ_t , and \mathcal{D}_f is the metric to measure the divergence between z_i^{t-1} and z_i^t . Fig. 4 illustrates our knowledge distillation learning framework.

Limitations of Prior Knowledge Distillation. Prior studies commonly adopted the Euclidean distance (ℓ_2) as a metric for \mathcal{D} to measure the feature discrepancy. However, using this metric in the continual learning paradigm could result in limited performance. In particular, using the constraint ℓ_2 as a regularization to each z_i^{t-1} and z_i^t , i.e. $\mathcal{D}_f(z_i^{t-1}, z_i^t) = \|z_i^t - z_i^{t-1}\|_2^2$ (where $\|\cdot\|_2^2$ is the ℓ_2 norm) could lead to the over-regularized problem. Although the ℓ_2 metric has shown efficiency in the close-problem (i.e., non-incremental learning), it can be sensitive to variations in features in continual learning due to its reliance on the absolute distances. When the model learns from new learning data, the scale of feature representations can change, leading to feature shifts that result in difficulty maintaining knowledge learned from previous steps.

The Proposed Angular-based Forgetting Mitigation (AFM). In the continual learning setting, imposing feature discrepancy via the direction, i.e., an angular metric, rather than magnitude, is more valuable for two reasons. First, the angular metric is more robust against the scale and noise of feature representations [122]. Second, since the downstream tasks commonly adopt the angular distances (e.g., fMRI-to-Image Retrieval [23, 27], fMRI-to-Image Synthesis [23, 24, 27, 28]) for computing similarity, using the angular metrics could further improve the performance on the downstream applications. Therefore, *the new angular metric is proposed to model the knowledge distillation as:*

$$\mathcal{D}_f(z_i^{t-1}, z_i^t) = \left\| 1 - \frac{z_i^{t-1}}{\|z_i^{t-1}\|} * \frac{z_i^t}{\|z_i^t\|} \right\|_2^2 \quad (7)$$

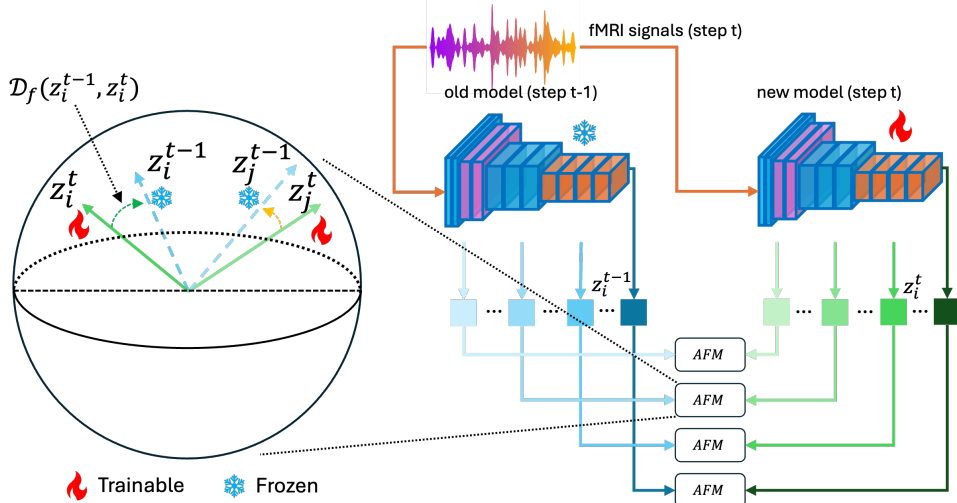


Fig. 4: Angular-based Forgetting Mitigation.

Under this form, our proposed distillation loss will maintain the knowledge of the model via the feature directions. Our learning approach produces a degree of freedom for the model to update the new knowledge during the current learning step.

4.5 Continual Vision-Brain Learning

At each learning step the vision-brain model F is learned with the **De-bias Contrastive Loss** defined in Eqn. (3) and the **Angular-based Forgetting Mitigation** presented in Eqn. (7). Formally, the entire bias-mitigation continual learning objective in our approach can be defined as in Eqn. (8).

$$\mathcal{L} = \mathcal{L}_C(x^t, y^t) + \lambda_{CL} \mathcal{L}_{CL}(x^t) = -\log \frac{\exp(z^t \times c^t)}{\sum_{z'} \exp(z' \times c^t)} e^{1-r(t)} + \lambda_{CL} \frac{1}{L} \sum \left\| 1 - \frac{z_i^{t-1}}{\|z_i^{t-1}\|} * \frac{z_i^t}{\|z_i^t\|} \right\|_2^2 \quad (8)$$

5 Datasets and Method Implementation

In this section, we begin by detailing the dataset used in our study and the evaluation protocol designed to test continual learning performance in the Section 5.1. The Natural Scenes Dataset (NSD) offers a unique opportunity to study fine-grained session-wise brain activity across multiple participants, making it particularly well-suited for continual learning research. Building on this dataset, we define an evaluation protocol that simulates real-world sequential training scenarios, where models must learn incrementally while retaining prior knowledge. This setup enables us to systematically investigate how different session splits and training strategies impact performance and memory retention. Next, we details the implementation and training hyperparameters used in our experiments in Section 5.2

5.1 Dataset and Evaluation Protocol

Dataset. We experiment on the Natural Scenes Dataset (NSD) [11]. It was collected from eight participants over multiple sessions, where each participant viewed a total of 73,000+ fMRI trials corresponding to 10,000 unique natural scene images sampled from the COCO dataset [123]. Each image was presented multiple times across different sessions, allowing researchers to analyze the reliability and consistency of brain responses. Each participant underwent extensive scanning (30-40 sessions per participant) while maintaining fixation on a central point. To the best of our knowledge, the NSD dataset is the only publicly available resource that provides fine-grained data collection session information, which is essential for establishing a continual learning setup. This temporal structure enables the study of session-wise signal bias and its effect on brain-vision understanding, as an aspect that is not supported by other existing datasets.

Evaluation Protocol. Let (N_{init}, N_s) denote a pair representing a Continual Learning (CL) setup, where N_{init} is the number of initial sessions used to train the initial model, and N_s is the number of sessions incorporated in each subsequent training step. At each training step, the model is initialized with the pre-trained weights from the previous step, if available. During evaluation, only test samples of the previous

and current sessions are used to measure the performance metric. Suppose we have $N_{session}$ data collection sessions. The total number of steps in the CL process is given by $\frac{N_{session}-N_{init}}{N_s} + 1$. We experiment with four CL setups: (20, 2), (20, 5), (20, 10), and (15, 5).

5.2 Implementation Details

fMRI Encoder and Vision Encoder. We employ an fMRI encoder similar to [23]. For Vision Encoder V , we utilize a pre-trained visual encoder from OpenCLIP models such as ViT-B/16 [124]. For our distillation loss, we use the features of $L = 3$ intermediate layers from the fMRI encoder.

Training Configuration. Our framework is implemented in PyTorch and trained on one NVIDIA A100 GPU. The learning rate is set to $2.5e^{-4}$ initially and then reduced to zero gradually with CosineLinear [125]. The CL weight factors λ_{CL} are set to 1. The model is optimized by AdamW [126] with a batch size of 16 for 50 epochs. The training is completed within two hours per subject.

6 Experimental Results

In this section, we firstly discuss the experimental results of average continual learning performance, as well as the individual’s performance on different continual learning setups. We also further do comprehensive ablation studies to analyze

6.1 Continual Learning Results

Table 4 provides an average continual learning performance and Fig. 5 details the performance on four subjects across different training settings on NSD. These results compare standard training without continual learning (W/o CL), Learning without Forgetting (LwF [127]), PLOP [119], and our proposed method under various incremental update configurations: (15, 5), (20, 10), (20, 2) and (20, 5). Across all settings, W/o CL exhibits a sharp decline in performance, confirming severe forgetting when learning new session data. For instance, in subject 01 under (20, 2), W/o CL achieves 61.57% at the first step (1–20), but 18.06% ($\downarrow 43.57\%$) at the end (39–40). Meanwhile, our proposed method achieves 57.97% ($\downarrow 3.6\%$). LwF and PLOP mitigate forgetting to some extent, but their effectiveness varies across settings. In particular, under (20, 2) setting, LwF achieves 54.7%, outperforming PLOP at 54.14%, but still lags behind our method at 57.97%. Our method consistently maintains higher accuracy in various subjects and learning settings, suggesting a more stable learning mechanism.

6.2 Ablation Studies

We report the average performance across all subjects in Table 2, while Fig. 6 illustrates the performance details of each subject.

Effectiveness of De-bias Contrastive Learning. We evaluate the effectiveness of DCL by comparing it with the baseline that uses vanilla Contrastive Learning. Here, DCL employs Response Accuracy (RA) to model the bias. To mitigate catastrophic forgetting, we incorporate ℓ_2 regularization. As shown in Table 2, the model trained

Table 1: Average continual learning performance across different settings (15, 5), (20, 10), (20, 2) and (20, 5) on NSD.

Method	(Brain \rightarrow Image) Retrieval																									
	(15, 5)						(20, 10)						(20, 2)						(20, 5)							
1-15	16-20	21-25	26-30	31-35	36-40	1-20	21-30	31-40	1-20	21-22	23-24	25-26	27-28	29-30	31-32	33-34	35-36	37-38	39-40	1-20	21-25	26-30	31-35	36-40		
W/o CL	49.64	30.24	30.2	29.32	29.43	28.75	54.3	40.8	38.89	54.62	17.95	17.6	17.37	17.7	16.91	16.14	16.29	17.11	17.83	16.28	52.56	31.05	30.26	29.78	29.58	
LvF	51.28	50.76	52.06	52.02	53.74	54.31	54.96	55.1	56.9	54.64	50.86	50.53	48.7	51.12	50.97	51.78	50.98	51.65	52.26	52.0	55.52	52.7	51.99	53.2	54.44	
PLOP	53.24	52.19	53.19	53.62	55.42	56.56	56.95	57.1	58.48	56.52	52.3	52.8	51.16	52.4	52.94	53.94	54.44	53.97	54.27	54.46	55.54	56.44	52.47	51.8	52.2	50.44
Ours	55.97	54.88	56.78	56.87	57.86	58.98	59.51	59.32	62.19	59.11	55.3	53.97	55.55	56.25	55.94	57.15	57.56	56.96	59.74	57.81	56.54	58.42	58.71			

Method	(Image \rightarrow Image) Retrieval																								
	(15, 5)						(20, 10)						(20, 2)						(20, 5)						
1-15	16-20	21-25	26-30	31-35	36-40	1-20	21-30	31-40	1-20	21-22	23-24	25-26	27-28	29-30	31-32	33-34	35-36	37-38	39-40	1-20	21-25	26-30	31-35	36-40	
W/o CL	44.52	26.44	25.5	24.33	25.24	24.81	48.31	36.15	34.41	48.26	13.58	12.57	13.9	13.68	13.11	12.86	12.52	12.77	13.03	11.89	46.42	25.6	25.36	24.89	24.72
LvF	45.64	41.18	46.45	46.03	47.46	48.85	49.29	49.32	51.8	49.09	43.4	42.98	41.31	41.96	41.75	41.45	41.75	43.52	45.83	45.34	49.44	46.21	46.55	47.24	49.05
PLOP	47.04	46.3	41.27	48.61	49.31	51.45	50.61	51.11	50.98	50.92	45.44	45.04	45.18	46.06	46.16	47.15	47.83	48.97	47.63	48.78	49.32	49.81	49.88	50.38	
Ours	50.64	49.25	50.44	51.51	51.97	53.62	54.61	53.95	56.72	53.72	48.37	49.6	48.82	48.86	49.27	50.39	49.23	51.15	50.85	50.64	53.97	51.37	51.02	52.55	54.06

Table 2: Ablation studies on the effectiveness of the proposed approach. Non-CL: Non Continual Learning. Contras: Contrastive Learning, RA: Response Accuracy, BA: Brain Activity, DCL: De-bias Contrastive Learning, AFM: Angular-based Forgetting Mitigation

Exp	Method	Alignment	forgetting	Rehearsal	(Brain \rightarrow Image) Retrieval																						
					(15, 5)						(20, 10)						(20, 2)						(20, 5)				
1-15	16-20	21-25	26-30	31-35	36-40	1-20	21-30	31-40	1-20	21-22	23-24	25-26	27-28	29-30	31-32	33-34	35-36	37-38	39-40	1-20	21-25	26-30	31-35	36-40			
1 Non-CL	Contras	ℓ_2	\times																								
2 Ours	Contras	ℓ_2	\times																								
3 Ours	DCL + RA	\times																									
4 Ours	DCL + RA	AFM	\checkmark																								
5 Ours	DCL + RA	AFM	\checkmark																								
6 Ours	DCL + RA	AFM	\checkmark																								

Exp	Method	Alignment	forgetting	Rehearsal	(Image \rightarrow Image) Retrieval																						
					(15, 5)						(20, 10)						(20, 2)						(20, 5)				
1-15	16-20	21-25	26-30	31-35	36-40	1-20	21-30	31-40	1-20	21-22	23-24	25-26	27-28	29-30	31-32	33-34	35-36	37-38	39-40	1-20	21-25	26-30	31-35	36-40			
1 Non-CL	Contras	ℓ_2	\times																								
2 Ours	Contras	ℓ_2	\times																								
3 Ours	DCL + RA	\times																									
4 Ours	DCL + RA	AFM	\checkmark																								
5 Ours	DCL + RA	AFM	\checkmark																								
6 Ours	DCL + RA	AFM	\checkmark																								

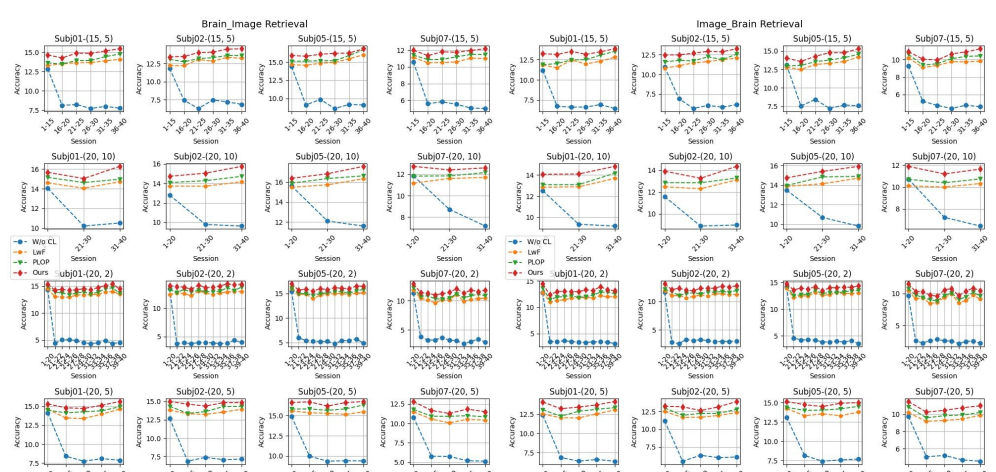


Fig. 5: Details continual learning performance of all subjects (subj01, subj02, subj05, and subj07) across different settings (15, 5), (20, 10), (20, 2), (20, 5), and retrieval tasks (Brain \rightarrow Image), (Image \rightarrow Brain).

These results demonstrate the superior performance of DCL over typical Contrastive Learning.

Effectiveness of Angular-based Forgetting Mitigation. We further assess the impact of AFM compared to ℓ_2 regularization. In this experiment, we use (DCL + RA) for alignment. As presented in Table 2, the model trained with (DCL + RA, AFM) in (Exp-6) achieves 1%-3% higher performance than (DCL + RA, ℓ_2) in (Exp-3) across the same subjects, continual learning setups, and retrieval tasks. This improvement suggests that AFM is more robust to noise than ℓ_2 , making it better suited for Vision-Brain Understanding tasks.

Non-Continual Learning Setting. In the Table 2, we compare our continual learning approach in (Exp-6) to the Non-Continual Learning (Non-CL) setup in (Exp-1), where data from all sessions is combined and trained in a single stage. The results show that our approach achieves competitive performance, surpassing the Non-CL setup—an uncommon outcome in other domains.

Modeling the Bias Factor. In Section 4.3, we proposed modeling the bias factor w^t using participants' accuracy responses during data collection, which tend to increase over sessions. Here, we explore an alternative approach to modeling this factor. Specifically, as participants experience uncertainty, their brain activity weakens, decreasing the number of activated voxels—i.e., voxels with values above zero. Motivated by this observation, we propose modeling $w^t = \frac{1}{p(t)}$ as: $w^t = e^{1-a(t)} = e^{1-N_a/N_b}$ where N_a represents the number of activated brain voxels, and N_b is the total number of brain voxels. Performance results are reported in Table 2. Overall, modeling the bias factor using Brain Activation (Exp - 4) yields slightly lower performance than the Accuracy Response (Exp - 6) approach. However, in practice, Accuracy Response may not always be available in certain datasets, whereas brain activity data is more accessible. Furthermore, Brain Activation-based modeling still outperforms previous methods such as LwF [127] and PLOP [119]. Therefore, in some cases, Brain Activity can serve as a viable alternative for modeling consistency in the brain.

Rehearsal-Free and Rehearsal-Based Approaches. In this section, we evaluate our proposed continual learning under a rehearsal-based approach. Specifically, after each training step t , we randomly retain 10% of the data and reuse it in the next step. Notably, we do not apply AFM in the rehearsal-based approach. The performance results are reported in Table 2. Our findings indicate that the rehearsal-based approach (Exp - 5) performs significantly worse than the rehearsal-free approach (Exp - 6) across various settings. It is because each sample pair forms an individual cluster, and retaining only 10% of the data prevents the loss of knowledge for those specific samples while potentially leading to the loss of information from the remaining 90%. For this reason, the rehearsal-based method is not an ideal solution for continual vision-brain understanding.

Comparison with SOTA in Brain-Image Retrieval. We compare our proposed approach with the SOTA method for the Brain-Image Retrieval task. For a fair comparison, we adopt the same model architecture and training strategy as MindEye [23], with the key difference being that we use the DCL loss instead of SoftCLIPLoss, as employed in their work. The performance results, presented in Table 3, show that our

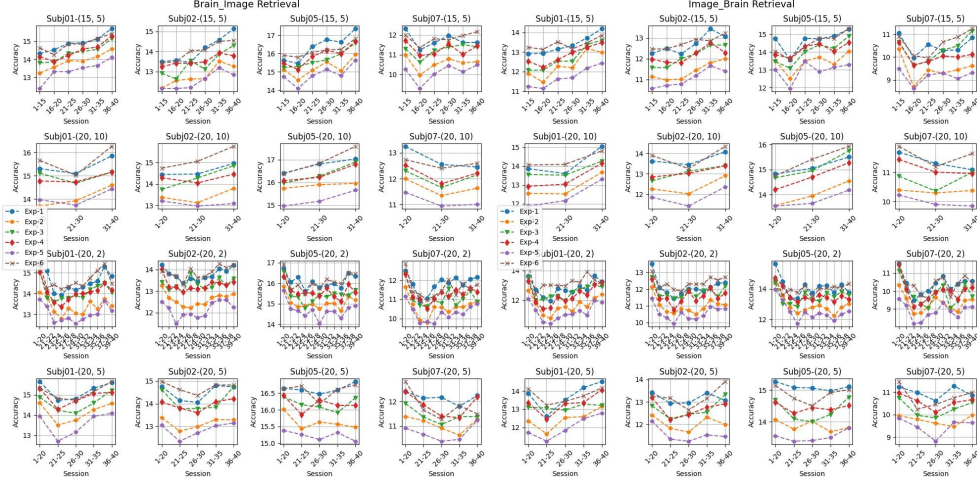


Fig. 6: Details ablation study performance of all subjects (subj01, subj02, subj05, and subj07) across different settings (15,5),(20,10),(20,2) and (20,5) on NSD. The detail settings of Exps1 – 6 can be found in Table 2

Table 3: Brain-Image retrieval results on the NSD.

Method	Image-Brain↑	Brain-Image↑
Lin et al. [128]	11.0%	49.0%
Ozcelik et al. [129]	21.1%	30.3%
MinD-Vis [130]	91.6%	85.9%
MindEye [23]	93.6%	90.1%
Ours	95.8%	95.3%

approach outperforms SOTA methods, demonstrating the effectiveness of the proposed DCL.

7 Conclusion

In this paper, we have presented the bias problem in brain signals caused by natural memory decay, where bias increases in later data collection sessions. We statistically and experimentally demonstrate the impact of this issue on vision-brain understanding models. Our analysis raises concerns about addressing this problem, as previous approaches have primarily overlooked. To tackle this problem, we have proposed a novel continual learning approach that enables the model to learn and adapt to the increasing bias across sessions. Specifically, we have introduced De-bias Contrastive Learning to mitigate bias and Angular-based Forgetting Mitigation to counteract catastrophic forgetting. Empirical results have demonstrated the effectiveness of our method in addressing bias in brain signals.

8 Data Availability

The data that support the findings of this study are openly available at <https://naturalscenesdataset.org/>.

9 Appendix

9.1 Details of Experiment Results: Continual Learning Comparison

Table 4: Continual Learning Performance on of NSD.

Method	subj01 - (Brain → Image) Retrieval																															
	(15, 5)					(20, 10)					(20, 2)					(20, 5)																
W/o CL	1-15	16-20	21-25	26-30	31-35	36-40	1-20	21-30	31-40	1-20	21-22	23-24	25-26	27-28	29-30	31-32	33-34	35-36	37-38	39-40	1-20	21-25	26-30	31-35	36-40							
	51.33	32.41	32.82	30.79	31.88	30.94	56.16	40.87	42.72	57.59	17.5	20.19	20.12	19.44	17.98	17.26	17.94	19.34	17.29	18.06	56.62	33.69	30.99	32.33	31.49							
	53.03	59.94	54.5	54.62	55.49	56.26	58.38	52.61	58.82	58.13	52.21	51.59	51.73	53.45	53.45	53.64	53.83	55.64	55.87	54.7	58.59	53.9	56.51	59.51	58.55	58.55						
	54.39	53.86	52.67	55.67	55.67	57.67	59.03	60.62	58.48	59.87	59.86	55.43	55.60	53.71	54.83	54.63	54.22	55.52	58.04	58.81	54.7	58.05	54.7	57.19	57.67	59.83	59.83					
	58.54	57.01	59.48	59.37	60.67	61.64	61.75	62.05	61.57	57.67	56.86	53.73	58.08	57.41	59.03	61.63	61.48	57.97	61.32	59.5	58.9	60.61	62.6									
	subj01 - (Image → Brain) Retrieval																															
	(15, 5)					(20, 10)					(20, 2)					(20, 5)																
	1-15	16-20	21-25	26-30	31-35	36-40	1-20	21-30	31-40	1-20	21-22	23-24	25-26	27-28	29-30	31-32	33-34	35-36	37-38	39-40	1-20	21-25	26-30	31-35	36-40							
	44.72	26.94	26.47	26.55	27.74	25.83	50.05	37.42	36.74	51.06	14.07	14.03	14.6	14.01	13.61	13.33	13.73	13.85	13.54	12.43	49.54	27.46	25.52	26.39	25.49							
	LwF	47.39	45.96	48.83	47.88	49.2	51.18	51.36	51.52	54.65	51.21	44.16	45.5	45.71	46.97	47.42	47.39	47.16	48.75	47.95	47.98	50.1	48.18	48.11	50.19	52.22						
	PLPO	47.45	48.05	49.92	49.66	52.22	54.07	52.33	52.33	56.63	54.38	46.0	47.67	48.25	47.89	47.41	48.91	51.58	51.44	52.33	49.40	51.56	52.59	53.43	53.43							
	Ours	52.94	52.55	54.07	52.63	53.87	55.37	56.23	56.35	59.22	57.75	49.5	52.3	52.08	51.96	51.84	53.25	52.76	55.61	53.55	52.48	56.42	52.9	53.73	54.9	56.65						
subj02 - (Brain → Image) Retrieval																																
W/o CL	(15, 5)					(20, 10)					(20, 2)					(20, 5)																
	1-15	16-20	21-25	26-30	31-35	36-40	1-20	21-30	31-40	1-20	21-22	23-24	25-26	27-28	29-30	31-32	33-34	35-36	37-38	39-40	1-20	21-25	26-30	31-35	36-40							
	W/o CL	47.39	29.72	25.2	29.88	28.85	27.5	51.16	39.13	38.47	53.75	15.28	15.69	15.12	15.87	15.87	15.63	15.12	15.56	17.4	16.04	50.83	27.58	29.68	28.37	28.77						
	LwF	48.91	48.89	52.29	51.36	54.84	53.0	54.9	54.85	56.63	49.7	50.43	50.35	48.74	51.80	50.47	50.64	51.4	51.59	51.75	52.35	52.52	52.95	54.2	55.69							
	PLPO	52.44	51.0	51.29	53.3	54.48	54.57	56.33	57.11	58.9	53.05	50.9	53.17	51.29	52.58	51.63	51.67	51.85	54.37	52.41	54.83	57.33	53.5	54.44	57.22	57.27						
	Ours	53.78	53.92	56.12	56.35	58.0	58.22	58.92	60.2	62.99	55.74	55.16	54.86	53.22	52.6	54.47	54.71	55.61	57.04	56.36	56.86	59.59	58.47	57.45	57.45	59.29	59.29					
subj02 - (Image → Brain) Retrieval																																
W/o CL	(15, 5)					(20, 10)					(20, 2)					(20, 5)																
	1-15	16-20	21-25	26-30	31-35	36-40	1-20	21-30	31-40	1-20	21-22	23-24	25-26	27-28	29-30	31-32	33-34	35-36	37-38	39-40	1-20	21-25	26-30	31-35	36-40							
	W/o CL	43.72	27.64	22.7	24.25	23.37	24.62	46.3	35.48	35.87	46.39	11.34	13.32	13.25	12.54	13.02	11.75	11.84	11.82	14.77	21.98	32.52	23.99	23.44	23.44							
	LwF	43.15	44.39	45.84	46.48	47.42	48.22	49.9	49.17	52.42	57.33	44.07	44.11	44.27	43.45	44.51	43.86	45.27	45.47	44.77	48.78	50.60	47.61	48.78	47.48	49.33						
	PLPO	46.33	47.41	48.63	48.43	49.8	50.23	51.43	51.37	53.13	48.57	45.67	46.76	44.08	45.33	46.08	45.19	46.56	47.41	46.3	47.63	52.40	47.87	48.86	49.43	51.23						
	Ours	49.86	49.9	50.72	51.73	51.44	52.98	55.64	53.02	57.4	52.45	48.24	49.44	47.92	47.45	49.22	49.18	49.23	50.8	50.12	50.87	52.99	52.68	50.55	52.62	55.65						
subj05 - (Image → Brain) Retrieval																																
W/o CL	(15, 5)					(20, 10)					(20, 2)					(20, 5)																
	1-15	16-20	21-25	26-30	31-35	36-40	1-20	21-30	31-40	1-20	21-22	23-24	25-26	27-28	29-30	31-32	33-34	35-36	37-38	39-40	1-20	21-25	26-30	31-35	36-40							
	W/o CL	42.33	23.29	22.7	22.95	20.4	41.4	36.7	28.5	45.49	45.29	15.23	15.06	13.13	12.24	12.02	12.01	13.17	11.56	14.59	23.23	23.02	20.49	20.39	20.39							
	LwF	44.55	41.87	42.08	43.35	41.01	44.65	46.4	47.02	44.98	48.85	44.92	44.85	44.26	43.91	43.51	43.74	41.39	41.55	45.91	41.21	40.27	42.08	41.76	41.76							
	PLPO	42.64	43.43	43.88	44.81	45.96	47.29	47.37	48.4	48.95	42.86	43.25	42.19	40.92	41.78	44.52	41.81	43.26	44.37	42.74	43.67	43.63	43.96	43.4								
	Ours	47.96	45.39	47.23	46.98	47.88	48.66	50.93	49.61	50.37	51.37	45.53	45.01	43.88	44.71	45.69	48.12	44.96	47.24	46.13	47.13	51.23	46.62	45.1	47.34	45.95						
subj07 - (Brain → Brain) Retrieval																																
W/o CL	(15, 5)					(20, 10)					(20, 2)					(20, 5)																
	1-15	16-20	21-25	26-30	31-35	36-40	1-20	21-30	31-40	1-20	21-22	23-24	25-26	27-28	29-30	31-32	33-34	35-36	37-38	39-40	1-20	21-25	26-30	31-35	36-40							
	W/o CL	37.22	20.97	19.09	17.66	19.13	18.44	42.92	28.53	25.76	38.66	10.46	8.8	10.56	11.31	10.4	10.24	8.65	10.03	10.28	8.82	39.84	20.28	20.91	18.82	18.23						

Table 4 presents the details of our experimental results for each subject in the continual learning setting.

9.2 Details of Experiment Results: Ablation Studies

Table 5 presents the detailed results of our ablative experiments for each subject.

9.3 Detail of Evaluation Metrics

To evaluate brain-to-image alignment, we follow the retrieval-based evaluation protocol introduced in the MindEye [23] and MindEye2 [27] studies. In Brain-Image retrieval, the task is to identify the correct image corresponding to an fMRI signal from a pool of candidate images. Specifically, given a test fMRI embedding, we compute its cosine similarity with the embeddings of a fixed number of candidate images (e.g.,

Table 5: Ablation Studies on various comparisons. Non-CL: Non Continual Learning. Contras: Contrastive Learning. L2: ℓ_2 : normalization, RA: Response Accuracy, BA: Brain Activity, DCL: De-bias Contrastive Learning, AFM: Angular-based Forgetting Mitigation

Exp	Method	Alignment	Forgetting	Rehearsed	subj01 - (Brain \rightarrow Image) Retrieval																									
					(15, 5)				(20, 10)				(20, 2)				(20, 5)													
1	Non-CL	Contras	\times		57.31	58.14	59.56	59.69	60.57	62.82	61.23	60.39	63.42	61.52	60.55	55.99	55.73	57.18	56.71	57.22	57.93	58.36	60.18	59.32	62.6	58.87	59.22	61.28	62.39	
2	Baseline	Contras	\times		52.97	54.24	55.77	55.58	56.63	58.28	54.8	57.78	55.21	57.82	51.58	52.7	52.01	54.51	53.07	55.0	53.67	58.38	54.03	54.96	57.05	58.28				
3	Ours	DCL + RA	\times		55.2	55.44	57.37	57.78	58.21	60.63	60.45	58.71	60.63	60.4	55.18	54.39	55.05	53.2	55.67	55.13	56.77	54.04	56.18	59.5	56.93	56.34	58.35	60.88		
4	Ours	DCL + RA	AFM		49.3	49.54	50.44	51.11	50.94	51.11	50.95	51.11	50.94	51.11	50.95	51.11	50.94	51.11	50.95	51.11	50.94	51.11	50.95	51.11	50.94	51.11	50.95	51.11	50.94	
5	Ours	DCL + RA	AFM	\checkmark	49.5	53.29	53.25	54.13	54.62	54.42	55.88	54.96	53.52	50.46	50.91	51.24	51.11	51.83	52.05	51.62	52.74	53.74	50.83	52.62	55.73	56.32				
6	Ours	DCL + RA	AFM	\times	58.54	59.1	59.48	59.13	60.64	61.75	62.65	60.12	65.06	61.57	57.69	58.86	57.33	58.88	57.41	59.0	60.43	61.68	57.97	61.32	59.3	58.9	60.61	62.6		
					subj01 - (Image \rightarrow Brain) Retrieval																									
Exp	Method	Alignment	Forgetting	Rehearsed	(15, 5)				(20, 10)				(20, 2)				(20, 5)													
					1-15	16-20	21-25	26-30	31-35	36-40	1-20	21-30	31-40	1-20	21-22	23-24	25-26	27-28	29-30	31-32	33-34	35-36	37-38	39-40	1-20	21-25	26-30	31-35	36-40	
1	Non-CL	Contras	\times		47.64	45.86	49.09	48.79	52.73	51.89	50.2	50.08	54.65	50.56	47.19	43.94	41.2	45.8	46.17	45.0	47.54	46.14	49.56	49.44	46.62	50.19	50.34	52.59		
2	Baseline	Contras	\times		48.3	48.32	50.13	50.14	53.58	54.35	54.19	54.07	57.02	54.04	48.8	48.2	49.04	49.2	47.84	50.21	51.61	52.43	52.24	51.77	53.12	52.84				
3	Ours	DCL + RA	\times		50.12	48.87	50.44	51.93	52.95	53.83	51.68	52.16	56.56	53.13	47.5	45.61	46.7	48.8	47.84	48.5	50.42	49.37	52.18	53.43	49.78	53.26	53.44	56.25		
4	Ours	DCL + RA	AFM		48.61	48.61	49.54	49.57	49.75	49.76	49.75	49.76	48.65	51.19	48.38	48.3	48.37	48.4	48.45	49.45	49.46	49.47	47.36	46.9	45.0	47.38	49.93	51.15		
5	Ours	DCL + RA	AFM	\checkmark	52.94	52.55	54.07	52.63	53.87	55.37	56.23	56.63	59.22	59.5	52.03	52.08	52.23	52.25	52.6	53.61	53.53	52.48	56.12	52.9	53.73	54.59	56.63			
					subj02 - (Brain \rightarrow Image) Retrieval																									
Exp	Method	Alignment	Forgetting	Rehearsed	(15, 5)				(20, 10)				(20, 2)				(20, 5)													
					1-15	16-20	21-25	26-30	31-35	36-40	1-20	21-30	31-40	1-20	21-22	23-24	25-26	27-28	29-30	31-32	33-34	35-36	37-38	39-40	1-20	21-25	26-30	31-35	36-40	
1	Non-CL	Contras	\times		53.95	54.26	53.77	54.78	58.32	60.53	57.75	57.84	58.68	55.25	54.68	53.49	54.35	53.8	54.51	54.69	56.15	55.72	56.76	59.02	56.56	59.18	58.97			
2	Baseline	Contras	\times		48.67	50.6	50.53	54.02	53.06	53.48	52.5	55.15	52.98	54.82	49.84	50.2	51.1	51.02	51.45	53.34	51.13	51.93	52.4	53.13	53.13	53.13	53.13	53.13		
3	Ours	DCL + RA	\times		50.12	50.53	51.33	51.44	52.04	52.05	52.05	52.05	52.05	52.05	52.05	52.05	52.05	52.05	52.05	52.05	52.05	52.05	52.05	52.05	52.05	52.05	52.05			
4	Ours	DCL + RA	AFM		52.92	53.68	54.64	55.16	55.74	56.18	56.04	52.76	52.72	51.81	52.55	52.3	52.59	53.68	53.51	53.12	53.68	52.59	52.22	54.39	56.32	56.88				
5	Ours	DCL + RA	AFM	\checkmark	48.61	48.61	49.54	49.57	50.63	51.21	51.53	50.84	48.74	49.58	47.66	47.66	47.38	47.38	47.38	47.38	47.38	47.38	47.38	47.38	47.38	47.38	47.38	47.38		
6	Ours	DCL + RA	AFM	\times	53.78	53.92	56.12	56.35	58.0	58.22	59.82	60.22	62.99	63.62	59.72	59.5	52.03	52.25	52.25	52.25	52.25	52.25	52.25	52.25	52.25	52.25	52.25	52.25	52.25	
					subj02 - (Image \rightarrow Brain) Retrieval																									
Exp	Method	Alignment	Forgetting	Rehearsed	(15, 5)				(20, 10)				(20, 2)				(20, 5)													
					1-15	16-20	21-25	26-30	31-35	36-40	1-20	21-30	31-40	1-20	21-22	23-24	25-26	27-28	29-30	31-32	33-34	35-36	37-38	39-40	1-20	21-25	26-30	31-35	36-40	
1	Non-CL	Contras	\times		60.48	60.23	61.26	60.23	63.77	62.98	63.84	60.17	59.39	59.57	58.89	59.02	60.11	58.64	61.4	60.71	64.04	61.73	62.54	62.27	61.92					
2	Baseline	Contras	\times		60.15	62.02	61.61	63.66	66.32	69.31	65.11	67.58	66.22	61.53	61.32	60.47	61.7	61.29	62.02	61.82	61.63	62.63	65.56	64.61	63.33	63.65	65.44			
3	Ours	DCL + RA	\times		61.87	60.5	63.33	64.72	63.96	66.67	64.31	64.91	67.19	65.31	62.54	61.89	62.11	62.07	61.64	63.04	61.67	65.71	63.42	65.19	64.5	64.5	64.5	64.5		
4	Ours	DCL + RA	AFM		58.94	56.34	59.13	60.52	62.53	59.86	60.71	62.61	64.72	64.72	64.72	64.72	64.72	64.72	64.72	64.72	64.72	64.72	64.72	64.72	64.72	64.72	64.72			
5	Ours	DCL + RA	AFM	\checkmark	42.98	42.87	43.13	44.76	46.63	45.63	45.47	45.67	44.51	44.51	44.51	44.51	44.51	44.51	44.51	44.51	44.51	44.51	44.51	44.51	44.51	44.51	44.51			
6	Ours	DCL + RA	AFM	\times	49.86	49.7	50.72	51.73	51.44	52.09	51.37	50.37	51.44	51.44	51.44	51.44	51.44	51.44	51.44	51.44	51.44	51.44	51.44	51.44	51.44	51.44	51.44			
					subj02 - (Image \rightarrow Brain) Retrieval																									
Exp	Method	Alignment	Forgetting	Rehearsed	(15, 5)				(20, 10)				(20, 2)				(20, 5)													
					1-15	16-20	21-25	26-30	31-35	36-40	1-20	21-30	31-40	1-20	21-22	23-24	25-26	27-28	29-30	31-32	33-34	35-36	37-38	39-40	1-20	21-25	26-30	31-35	36-40	
1	Non-CL	Contras	\times		44.92	44.95	46.41	47.84	46.45	46.49	52.99	50.2	49.8	50.0	47.19	43.7	44.16	46.63	48.05	47.42	48.5	47.42	48.5	49.61	48.54	48.67	47.05	48.55		
2	Baseline	Contras	\times		45.26	42.26	44.47	44.54	45.58	45.26	45.49	45.02	46.03	46.27	46.58	47.36	47.42	47.86	47.21	48.7	47.55	47.55	47.55	47.55	47.55	47.55	47.55	47.55		
3	Ours	DCL + RA	\times		42.57	42.86</																								

9.4 Limitations

One limitation of our study is that the analysis and validation of representation bias in brain signals are based solely on the NSD [11] dataset, which may raise concerns about the generalizability of our findings to other neuroimaging datasets. However, NSD is currently the largest and most comprehensive publicly available fMRI dataset for natural scene viewing, and notably, it is the only one that provides fine-grained session-level information along with human behavioral responses over long-term repeated measurements. These unique characteristics make NSD particularly well suited for studying temporal bias and session-dependent signal representation which is an essential requirement for establishing and evaluating continual learning setups in visual-brain understanding.

9.5 Broader Impacts

Advances in deep learning and neuroscience show the way for more adaptive and long-term applications of fMRI. Our proposed Bias-Mitigation Continual Learning (BRAIN) framework addresses a critical challenge in this direction: the session-wise representation bias that arises as brain signals change over time. By explicitly modeling and adapting to this temporal drift, our approach enables more stable and generalizable learning from fMRI data. This is especially important for future applications such as brain-image retrieval, reconstructing visual experiences, decoding internal speech, and developing neural prosthetics for communication where the ability to continuously learn from and adapt to evolving brain signals is essential.

References

- [1] Van Essen, D.C., Anderson, C.H., Felleman, D.J.: Information processing in the primate visual system: an integrated systems perspective. *Science* **255**(5043), 419–423 (1992)
- [2] Tsao, D.Y., Freiwald, W.A., Tootell, R.B., Livingstone, M.S.: A cortical region consisting entirely of face-selective cells. *Science* **311**(5761), 670–674 (2006)
- [3] Liang, L., Fratzl, A., Goldey, G., Ramesh, R.N., Sugden, A.U., Morgan, J.L., Chen, C., Andermann, M.L.: A fine-scale functional logic to convergence from retina to thalamus. *Cell* **173**(6), 1343–1355 (2018)
- [4] Wang, G., Tanaka, K., Tanifuchi, M.: Optical imaging of functional organization in the monkey inferotemporal cortex. *Science* **272**(5268), 1665–1668 (1996)
- [5] Raichle, M.E., MacLeod, A.M., Snyder, A.Z., Powers, W.J., Gusnard, D.A., Shulman, G.L.: A default mode of brain function. *Proceedings of the national academy of sciences* **98**(2), 676–682 (2001)
- [6] Hubel, D.H., Wiesel, T.N., *et al.*: Receptive fields of single neurones in the cat's striate cortex. *J physiol* **148**(3), 574–591 (1959)
- [7] Nauhaus, I., Nielsen, K.J., Disney, A.A., Callaway, E.M.: Orthogonal micro-organization of orientation and spatial frequency in primate primary visual cortex. *Nature neuroscience* **15**(12), 1683–1690 (2012)
- [8] Livingstone, M.S., Hubel, D.H.: Anatomy and physiology of a color system in the primate visual cortex. *Journal of Neuroscience* **4**(1), 309–356 (1984)
- [9] Posner, M.I., Snyder, C.R., Davidson, B.J.: Attention and the detection of signals. *Journal of experimental psychology: General* **109**(2), 160 (1980)
- [10] Hubel, D.H., Wiesel, T.N.: Receptive fields and functional architecture of monkey striate cortex. *The Journal of physiology* **195**(1), 215–243 (1968)
- [11] Allen, E.J., St-Yves, G., Wu, Y., Breedlove, J.L., Prince, J.S., Dowdle, L.T., Nau, M., Caron, B., Pestilli, F., Charest, I., *et al.*: A massive 7t fmri dataset to bridge cognitive neuroscience and artificial intelligence. *Nature neuroscience* **25**(1), 116–126 (2022)
- [12] Hebart, M.N., Contier, O., Teichmann, L., Rockter, A.H., Zheng, C.Y., Kidder, A., Corriveau, A., Vaziri-Pashkam, M., Baker, C.I.: Things-data, a multimodal collection of large-scale datasets for investigating object representations in human brain and behavior. *Elife* **12**, 82580 (2023)
- [13] Boyle, J.A., Pinsard, B., Boukhadir, A., Belleville, S., Brambatti, S., Chen, J., Cohen-Adad, J., Cyr, A., Fuente Rainville, P., Bellec, P.: The courtois

project on neuronal modelling-first data release. In: 26th Annual Meeting of the Organization for Human Brain Mapping (2020)

[14] Block, N.: Perceptual consciousness overflows cognitive access. *Trends in cognitive sciences* **15**(12), 567–575 (2011)

[15] Buschman, T.J., Siegel, M., Roy, J.E., Miller, E.K.: Neural substrates of cognitive capacity limitations. *Proceedings of the National Academy of Sciences* **108**(27), 11252–11255 (2011)

[16] Cohen, M.A., Dennett, D.C., Kanwisher, N.: What is the bandwidth of perceptual experience? *Trends in cognitive sciences* **20**(5), 324–335 (2016)

[17] Pylyshyn, Z.: Is vision continuous with cognition?: The case for cognitive impenetrability of visual perception. *Behavioral and brain sciences* **22**(3), 341–365 (1999)

[18] Whitney, D., Yamanashi Leib, A.: Ensemble perception. *Annual review of psychology* **69**(1), 105–129 (2018)

[19] Luck, S.J., Vogel, E.K.: Visual working memory capacity: from psychophysics and neurobiology to individual differences. *Trends in cognitive sciences* **17**(8), 391–400 (2013)

[20] Ozcelik, F., Choksi, B., Mozafari, M., Reddy, L., VanRullen, R.: Reconstruction of perceived images from fmri patterns and semantic brain exploration using instance-conditioned gans. In: 2022 International Joint Conference on Neural Networks (IJCNN), pp. 1–8 (2022). IEEE

[21] Shen, G., Horikawa, T., Majima, K., Kamitani, Y.: Deep image reconstruction from human brain activity. *PLoS computational biology* **15**(1), 1006633 (2019)

[22] Takagi, Y., Nishimoto, S.: High-resolution image reconstruction with latent diffusion models from human brain activity. In: Proceedings of the IEEE/CVF Conference on Computer Vision and Pattern Recognition, pp. 14453–14463 (2023)

[23] Scotti, P., Banerjee, A., Goode, J., Shabalin, S., Nguyen, A., Dempster, A., Verlinde, N., Yundler, E., Weisberg, D., Norman, K., et al.: Reconstructing the mind’s eye: fmri-to-image with contrastive learning and diffusion priors. *Advances in Neural Information Processing Systems* **36** (2024)

[24] Wang, S., Liu, S., Tan, Z., Wang, X.: Mindbridge: A cross-subject brain decoding framework. In: Proceedings of the IEEE/CVF Conference on Computer Vision and Pattern Recognition, pp. 11333–11342 (2024)

[25] Quan, R., Wang, W., Tian, Z., Ma, F., Yang, Y.: Psychometry: An omnifit

model for image reconstruction from human brain activity. In: Proceedings of the IEEE/CVF Conference on Computer Vision and Pattern Recognition, pp. 233–243 (2024)

- [26] Huo, J., Wang, Y., Qian, X., Wang, Y., Li, C., Feng, J., Fu, Y.: Neuropictor: Refining fmri-to-image reconstruction via multi-individual pretraining and multi-level modulation. arXiv preprint arXiv:2403.18211 (2024)
- [27] Scotti, P.S., Tripathy, M., Villanueva, C.K.T., Kneeland, R., Chen, T., Narang, A., Santhirasegaran, C., Xu, J., Naselaris, T., Norman, K.A., et al.: Mindeye2: Shared-subject models enable fmri-to-image with 1 hour of data. arXiv preprint arXiv:2403.11207 (2024)
- [28] Xia, W., Charette, R., Öztireli, C., Xue, J.-H.: UMBRAE: Unified Multimodal Brain Decoding (2024). <https://arxiv.org/abs/2404.07202>
- [29] Aflalo, T., Kellis, S., Klaes, C., Lee, B., Shi, Y., Pejsa, K., Shanfield, K., Hayes-Jackson, S., Aisen, M., Heck, C., et al.: Decoding motor imagery from the posterior parietal cortex of a tetraplegic human. *Science* **348**(6237), 906–910 (2015)
- [30] Bai, Y., Wang, X., Cao, Y.-p., Ge, Y., Yuan, C., Shan, Y.: Dreamdiffusion: Generating high-quality images from brain eeg signals. arXiv preprint arXiv:2306.16934 (2023)
- [31] Nguyen, X.-B., Duong, C.N., Li, X., Gauch, S., Seo, H.-S., Luu, K.: Micron-bert: Bert-based facial micro-expression recognition. In: Proceedings of the Ieee/cvf Conference on Computer Vision and Pattern Recognition, pp. 1482–1492 (2023)
- [32] Nguyen, X.-B., Bui, D.T., Duong, C.N., Bui, T.D., Luu, K.: Clusformer: A transformer based clustering approach to unsupervised large-scale face and visual landmark recognition. In: Proceedings of the IEEE/CVF Conference on Computer Vision and Pattern Recognition, pp. 10847–10856 (2021)
- [33] Nguyen, X.-B., Lee, G.S., Kim, S.H., Yang, H.J.: Self-supervised learning based on spatial awareness for medical image analysis. *IEEE Access* **8**, 162973–162981 (2020)
- [34] Nguyen, P., Quach, K.G., Duong, C.N., Le, N., Nguyen, X.-B., Luu, K.: Multi-camera multiple 3d object tracking on the move for autonomous vehicles. In: Proceedings of the IEEE/CVF Conference on Computer Vision and Pattern Recognition, pp. 2569–2578 (2022)
- [35] Nguyen, H.-Q., Truong, T.-D., Nguyen, X.B., Dowling, A., Li, X., Luu, K.: Insect-foundation: A foundation model and large-scale 1m dataset for visual insect understanding. In: Proceedings of the IEEE/CVF Conference on Computer Vision and Pattern Recognition, pp. 21945–21955 (2024)

- [36] Nguyen, X.-B., Nguyen, H.-Q., Chen, S.Y.-C., Khan, S.U., Churchill, H., Luu, K.: Qclusformer: A quantum transformer-based framework for unsupervised visual clustering. arXiv preprint arXiv:2405.19722 (2024)
- [37] Truong, T.-D., Chappa, R.T.N., Nguyen, X.-B., Le, N., Dowling, A.P., Luu, K.: Otadapt: Optimal transport-based approach for unsupervised domain adaptation. In: 2022 26th International Conference on Pattern Recognition (ICPR), pp. 2850–2856 (2022). IEEE
- [38] Nguyen, H.-Q., Nguyen, X.B., Chen, S.Y.-C., Churchill, H., Borys, N., Khan, S.U., Luu, K.: Diffusion-inspired quantum noise mitigation in parameterized quantum circuits. arXiv preprint arXiv:2406.00843 (2024)
- [39] Nguyen, X.B., Churchill, H., Luu, K., Khan, S.U.: Quantum vision clustering. arXiv preprint arXiv:2309.09907 (2023)
- [40] Nguyen, X.B., Bisht, A., Churchill, H., Luu, K.: Two-dimensional quantum material identification via self-attention and soft-labeling in deep learning. arXiv preprint arXiv:2205.15948 (2022)
- [41] Nguyen, X.-B., Nguyen, H.-Q., Churchill, H., Khan, S.U., Luu, K.: Quantum visual feature encoding revisited. *Quantum Machine Intelligence* **6**(2), 61 (2024)
- [42] Nguyen, X.-B., Duong, C.N., Savvides, M., Roy, K., Churchill, H., Luu, K.: Fairness in visual clustering: A novel transformer clustering approach. arXiv preprint arXiv:2304.07408 (2023)
- [43] Nguyen, X.-B., Li, X., Khan, S.U., Luu, K.: Brainformer: Modeling mri brain functions to machine vision. arXiv preprint arXiv:2312.00236 (2023)
- [44] Nguyen-Xuan, B., Lee, G.-S.: Sketch recognition using lstm with attention mechanism and minimum cost flow algorithm. *International Journal of Contents* **15**(4), 8–15 (2019)
- [45] Xia, W., Oztireli, C.: Exploring the visual feature space for multimodal neural decoding. arXiv preprint arXiv:2505.15755 (2025)
- [46] Nguyen, X.-B., Liu, X., Li, X., Luu, K.: The algonauts project 2023 challenge: Uark-ualbany team solution. arXiv preprint arXiv:2308.00262 (2023)
- [47] Nguyen, X.-B., Lee, G.-S., Kim, S.-H., Yang, H.-J.: Audio-video based emotion recognition using minimum cost flow algorithm. In: 2019 IEEE/CVF International Conference on Computer Vision Workshop (ICCVW), pp. 3737–3741 (2019). IEEE
- [48] Nguyen, X.-B., Nguyen, H.-Q., Churchill, H., Khan, S.U., Luu, K.: Hierarchical quantum control gates for functional mri understanding. arXiv preprint

arXiv:2408.03596 (2024)

- [49] Truong, T.-D., Nguyen, H.-Q., Nguyen, X.-B., Dowling, A., Li, X., Luu, K.: Insect-foundation: A foundation model and large multimodal dataset for vision-language insect understanding. *International Journal of Computer Vision*, 1–26 (2025)
- [50] Nguyen, H.-Q., Nguyen, X.-B., Churchill, H., Choudhary, A.K., Sinha, P., Khan, S.U., Luu, K.: Quantum-brain: Quantum-inspired neural network approach to vision-brain understanding. arXiv preprint arXiv:2411.13378 (2024)
- [51] Nguyen, X.-B., Jang, H., Li, X., Khan, S.U., Sinha, P., Luu, K.: Bractive: A brain activation approach to human visual brain learning. arXiv preprint arXiv:2405.18808 (2024)
- [52] Nguyen, X.-B., Choudhary, A.K., Sinha, P., Li, X., Luu, K.: Cobra: A continual learning approach to vision-brain understanding. arXiv preprint arXiv:2411.17475 (2024)
- [53] Belyi, R., Gaziv, G., Hoogi, A., Strappini, F., Golan, T., Irani, M.: From voxels to pixels and back: Self-supervision in natural-image reconstruction from fmri. *Advances in Neural Information Processing Systems* **32** (2019)
- [54] Fang, T., Zheng, Q., Pan, G.: Alleviating the semantic gap for generalized fmri-to-image reconstruction. *Advances in Neural Information Processing Systems* **36**, 15096–15107 (2023)
- [55] Chen, H., He, L., Liu, Y., Yang, L.: Visual neural decoding via improved visual-eeg semantic consistency. arXiv preprint arXiv:2408.06788 (2024)
- [56] Du, C., Fu, K., Li, J., He, H.: Decoding visual neural representations by multi-modal learning of brain-visual-linguistic features. *IEEE Transactions on Pattern Analysis and Machine Intelligence* **45**(9), 10760–10777 (2023)
- [57] Li, D., Wei, C., Li, S., Zou, J., Qin, H., Liu, Q.: Visual decoding and reconstruction via eeg embeddings with guided diffusion. arXiv preprint arXiv:2403.07721 (2024)
- [58] Song, Y., Liu, B., Li, X., Shi, N., Wang, Y., Gao, X.: Decoding natural images from eeg for object recognition. arXiv preprint arXiv:2308.13234 (2023)
- [59] Radford, A., Kim, J.W., Hallacy, C., Ramesh, A., Goh, G., Agarwal, S., Sastry, G., Askell, A., Mishkin, P., Clark, J., *et al.*: Learning transferable visual models from natural language supervision. In: *International Conference on Machine Learning*, pp. 8748–8763 (2021). PMLR
- [60] Sohl-Dickstein, J., Weiss, E.A., Maheswaranathan, N., Ganguli, S.: Deep

unsupervised learning using nonequilibrium thermodynamics. CoRR [abs/1503.03585](https://arxiv.org/abs/1503.03585) (2015) [1503.03585](https://arxiv.org/abs/1503.03585)

- [61] Ho, J., Jain, A., Abbeel, P.: Denoising diffusion probabilistic models. arXiv preprint arxiv:2006.11239 (2020)
- [62] Dhariwal, P., Nichol, A.: Diffusion models beat gans on image synthesis. CoRR [abs/2105.05233](https://arxiv.org/abs/2105.05233) (2021) [2105.05233](https://arxiv.org/abs/2105.05233)
- [63] Rombach, R., Blattmann, A., Lorenz, D., Esser, P., Ommer, B.: High-Resolution Image Synthesis with Latent Diffusion Models (2022). <https://arxiv.org/abs/2112.10752>
- [64] Xu, X., Wang, Z., Zhang, E., Wang, K., Shi, H.: Versatile Diffusion: Text, Images and Variations All in One Diffusion Model (2024). <https://arxiv.org/abs/2211.08332>
- [65] Wang, Z., Zhang, Z., Lee, C.-Y., Zhang, H., Sun, R., Ren, X., Su, G., Perot, V., Dy, J., Pfister, T.: Learning to Prompt for Continual Learning (2022). <https://arxiv.org/abs/2112.08654>
- [66] Hayes, T.L., Cahill, N.D., Kanan, C.: Memory Efficient Experience Replay for Streaming Learning (2019). <https://arxiv.org/abs/1809.05922>
- [67] Chaudhry, A., Rohrbach, M., Elhoseiny, M., Ajanthan, T., Dokania, P.K., Torr, P.H.S., Ranzato, M.: On Tiny Episodic Memories in Continual Learning (2019). <https://arxiv.org/abs/1902.10486>
- [68] Chaudhry, A., Gordo, A., Dokania, P.K., Torr, P., Lopez-Paz, D.: Using Hind-sight to Anchor Past Knowledge in Continual Learning (2021). <https://arxiv.org/abs/2002.08165>
- [69] Chaudhry, A., Ranzato, M., Rohrbach, M., Elhoseiny, M.: Efficient Lifelong Learning with A-GEM (2019). <https://arxiv.org/abs/1812.00420>
- [70] Buzzega, P., Boschini, M., Porrello, A., Abati, D., Calderara, S.: Dark Experience for General Continual Learning: a Strong, Simple Baseline (2020). <https://arxiv.org/abs/2004.07211>
- [71] Rebuffi, S.-A., Kolesnikov, A., Sperl, G., Lampert, C.H.: iCaRL: Incremental Classifier and Representation Learning (2017). <https://arxiv.org/abs/1611.07725>
- [72] Shokri, R., Shmatikov, V.: Privacy-preserving deep learning. In: 2015 53rd Annual Allerton Conference on Communication, Control, and Computing (Allerton), pp. 909–910 (2015). <https://doi.org/10.1109/ALLERTON.2015.7447103>
- [73] Pham, Q., Liu, C., Hoi, S.: DualNet: Continual Learning, Fast and Slow (2021).

<https://arxiv.org/abs/2110.00175>

- [74] Cha, H., Lee, J., Shin, J.: Co2l: Contrastive continual learning. In: Proceedings of the IEEE/CVF International Conference on Computer Vision, pp. 9516–9525 (2021)
- [75] Wu, Y., Chen, Y., Wang, L., Ye, Y., Liu, Z., Guo, Y., Fu, Y.: Large Scale Incremental Learning (2019). <https://arxiv.org/abs/1905.13260>
- [76] Wang, K., Herranz, L., Weijer, J.: Continual learning in cross-modal retrieval. In: Proceedings of the IEEE/CVF Conference on Computer Vision and Pattern Recognition, pp. 3628–3638 (2021)
- [77] Liu, W., Zhu, F., Wei, L., Tian, Q.: C-clip: Multimodal continual learning for vision-language model. In: The Thirteenth International Conference on Learning Representations (2025)
- [78] Cai, Y., Bi, K., Fan, Y., Guo, J., Chen, W., Cheng, X.: L2r: Lifelong learning for first-stage retrieval with backward-compatible representations. In: Proceedings of the 32nd ACM International Conference on Information and Knowledge Management, pp. 183–192 (2023)
- [79] Wan, T.S., Chen, J.-C., Wu, T.-Y., Chen, C.-S.: Continual learning for visual search with backward consistent feature embedding. In: Proceedings of the IEEE/CVF Conference on Computer Vision and Pattern Recognition, pp. 16702–16711 (2022)
- [80] Cui, Z., Zhou, J., Wang, X., Zhu, M., Peng, Y.: Learning continual compatible representation for re-indexing free lifelong person re-identification. In: Proceedings of the IEEE/CVF Conference on Computer Vision and Pattern Recognition, pp. 16614–16623 (2024)
- [81] Liu, S., Yang, Y., Li, X., Clifton, D.A., Ghanem, B.: Enhancing online continual learning with plug-and-play state space model and class-conditional mixture of discretization. arXiv preprint arXiv:2412.18177 (2024)
- [82] Wu, K., Li, X., Li, X., Hu, C., Wu, G.: Avqacl: A novel benchmark for audio-visual question answering continual learning
- [83] Zhou, Y., Tian, Y., Lv, J., Shi, M., Li, Y., Ye, Q., Zhang, S., Lv, J.: Ferret: An efficient online continual learning framework under varying memory constraints. arXiv preprint arXiv:2503.12053 (2025)
- [84] Wang, H., Lu, H., Yao, L., Gong, D.: Self-expansion of pre-trained models with mixture of adapters for continual learning. arXiv preprint arXiv:2403.18886 (2024)

- [85] Yu, L., Han, H., Tao, Z., Yao, H., Xu, C.: Language guided concept bottleneck models for interpretable continual learning. arXiv preprint arXiv:2503.23283 (2025)
- [86] Hu, Y., Liang, Z., Yang, F., Hou, Q., Liu, X., Cheng, M.-M.: Kac: Kolmogorov-arnold classifier for continual learning. arXiv preprint arXiv:2503.21076 (2025)
- [87] Liu, X., Chang, X.: Lora subtraction for drift-resistant space in exemplar-free continual learning. arXiv preprint arXiv:2503.18985 (2025)
- [88] Yu, H., Yang, X., Zhang, L., Gu, H., Li, T., Fan, L., Yang, Q.: Addressing spatial-temporal data heterogeneity in federated continual learning via tail anchor. arXiv preprint arXiv:2412.18355 (2024)
- [89] Kang, H., Seifer, G., Lee, D., Ryu, J.: Do your best and get enough rest for continual learning. arXiv preprint arXiv:2503.18371 (2025)
- [90] Wu, H., Li, Q., Zhang, C., He, Z., Ying, X.: Bridging the vision-brain gap with an uncertainty-aware blur prior. arXiv preprint arXiv:2503.04207 (2025)
- [91] Tran, Q., Tran, T.L., Doan, K., Tran, T., Phung, D., Than, K., Le, T.: Boosting multiple views for pretrained-based continual learning. In: The Thirteenth International Conference on Learning Representations (2025)
- [92] Resani, H., Nasihatkon, B.: Miracle 3d: Memory-efficient integrated robust approach for continual learning on point clouds via shape model construction. arXiv preprint arXiv:2410.06418 (2024)
- [93] Serra, G., Buettner, F.: Federated continual learning goes online: Uncertainty-aware memory management for vision tasks and beyond. arXiv preprint arXiv:2405.18925 (2024)
- [94] Seo, M., Koh, H., Choi, J.: Budgeted online continual learning by adaptive layer freezing and frequency-based sampling. arXiv preprint arXiv:2410.15143 (2024)
- [95] Peng, L., Elenter, J., Agterberg, J., Ribeiro, A., Vidal, R.: Tsvd: Bridging theory and practice in continual learning with pre-trained models. In: The Thirteenth International Conference on Learning Representations (2025)
- [96] Eskandar, M., Imtiaz, T., Hill, D., Wang, Z., Dy, J.: Star: Stability-inducing weight perturbation for continual learning. arXiv preprint arXiv:2503.01595 (2025)
- [97] Zhou, Y., Zhao, S., Wang, J., Jiang, H., Li, S., Li, T., Pan, G.: Brainuicl: An unsupervised individual continual learning framework for eeg applications. In: The Thirteenth International Conference on Learning Representations

[98] Chen, H., Goldblum, M., Wu, Z., Jiang, Y.-G.: Adaptive retention & correction: Test-time training for continual learning. In: The Thirteenth International Conference on Learning Representations

[99] Woo, S., Yun, J., Kim, G.: Meta-continual learning of neural fields. arXiv preprint arXiv:2504.05806 (2025)

[100] Salami, R., Buzzega, P., Mosconi, M., Bonato, J., Sabetta, L., Calderara, S.: Closed-form merging of parameter-efficient modules for federated continual learning. arXiv preprint arXiv:2410.17961 (2024)

[101] Ma'sum, M.A., Pratama, M., Ramasamy, S., Liu, L., Habibullah, H., Kowalczyk, R.: Vision and language synergy for rehearsal free continual learning. In: The Thirteenth International Conference on Learning Representations (2025)

[102] Park, J., Park, D., Lee, J.-G.: Active learning for continual learning: Keeping the past alive in the present. arXiv preprint arXiv:2501.14278 (2025)

[103] Farias, V.F., Jozefiak, A.D.: Self-normalized resets for plasticity in continual learning. arXiv preprint arXiv:2410.20098 (2024)

[104] Zheng, J., Cai, X., Qiu, S., Ma, Q.: Spurious forgetting in continual learning of language models. arXiv preprint arXiv:2501.13453 (2025)

[105] Ven, G.M.: On the computation of the fisher information in continual learning. arXiv preprint arXiv:2502.11756 (2025)

[106] Zhao, T., Wang, Z., Masoomi, A., Dy, J.: Deep Bayesian Unsupervised Lifelong Learning (2021). <https://arxiv.org/abs/2106.07035>

[107] Yoon, J., Yang, E., Lee, J., Hwang, S.J.: Lifelong Learning with Dynamically Expandable Networks (2018). <https://arxiv.org/abs/1708.01547>

[108] Rusu, A.A., Rabinowitz, N.C., Desjardins, G., Soyer, H., Kirkpatrick, J., Kavukcuoglu, K., Pascanu, R., Hadsell, R.: Progressive Neural Networks (2022). <https://arxiv.org/abs/1606.04671>

[109] Rao, D., Visin, F., Rusu, A.A., Teh, Y.W., Pascanu, R., Hadsell, R.: Continual Unsupervised Representation Learning (2019). <https://arxiv.org/abs/1910.14481>

[110] Loo, N., Swaroop, S., Turner, R.E.: Generalized Variational Continual Learning (2020). <https://arxiv.org/abs/2011.12328>

[111] Li, X., Zhou, Y., Wu, T., Socher, R., Xiong, C.: Learn to Grow: A Continual Structure Learning Framework for Overcoming Catastrophic Forgetting (2019). <https://arxiv.org/abs/1904.00310>

- [112] Wortsman, M., Ramanujan, V., Liu, R., Kembhavi, A., Rastegari, M., Yosinski, J., Farhadi, A.: Supermasks in Superposition (2020). <https://arxiv.org/abs/2006.14769>
- [113] Serrà, J., Surís, D., Miron, M., Karatzoglou, A.: Overcoming catastrophic forgetting with hard attention to the task (2018). <https://arxiv.org/abs/1801.01423>
- [114] Mallya, A., Lazebnik, S.: PackNet: Adding Multiple Tasks to a Single Network by Iterative Pruning (2018). <https://arxiv.org/abs/1711.05769>
- [115] Ke, Z., Liu, B., Huang, X.: Continual Learning of a Mixed Sequence of Similar and Dissimilar Tasks (2021). <https://arxiv.org/abs/2112.10017>
- [116] Truong, T.-D., Prabhu, U., Raj, B., Cothren, J., Luu, K.: Falcon: Fairness learning via contrastive attention approach to continual semantic scene understanding. arXiv preprint arXiv:2311.15965 (2023)
- [117] Cui, J., Zhong, Z., Liu, S., Yu, B., Jia, J.: Parametric contrastive learning. In: Proceedings of the IEEE/CVF International Conference on Computer Vision, pp. 715–724 (2021)
- [118] Cui, J., Zhong, Z., Tian, Z., Liu, S., Yu, B., Jia, J.: Generalized parametric contrastive learning. IEEE Transactions on Pattern Analysis and Machine Intelligence (2023)
- [119] Douillard, A., Chen, Y., Dapogny, A., Cord, M.: Plop: Learning without forgetting for continual semantic segmentation. In: Proceedings of the IEEE/CVF Conference on Computer Vision and Pattern Recognition, pp. 4040–4050 (2021)
- [120] Kirkpatrick, J., Pascanu, R., Rabinowitz, N., Veness, J., Desjardins, G., Rusu, A.A., Milan, K., Quan, J., Ramalho, T., Grabska-Barwinska, A., *et al.*: Overcoming catastrophic forgetting in neural networks. Proceedings of the national academy of sciences **114**(13), 3521–3526 (2017)
- [121] Zhang, C.-B., Xiao, J.-W., Liu, X., Chen, Y.-C., Cheng, M.-M.: Representation compensation networks for continual semantic segmentation. In: Proceedings of the IEEE/CVF Conference on Computer Vision and Pattern Recognition, pp. 7053–7064 (2022)
- [122] Deng, J., Guo, J., Xue, N., Zafeiriou, S.: Arcface: Additive angular margin loss for deep face recognition. In: Proceedings of the IEEE/CVF Conference on Computer Vision and Pattern Recognition, pp. 4690–4699 (2019)
- [123] Lin, T.-Y., Maire, M., Belongie, S., Hays, J., Perona, P., Ramanan, D., Dollár, P., Zitnick, C.L.: Microsoft coco: Common objects in context. In: Computer Vision–ECCV 2014: 13th European Conference, Zurich, Switzerland, September

6-12, 2014, Proceedings, Part V 13, pp. 740–755 (2014). Springer

- [124] Radford, A., Kim, J.W., Hallacy, C., Ramesh, A., Goh, G., Agarwal, S., Sastry, G., Askell, A., Mishkin, P., Clark, J., Krueger, G., Sutskever, I.: Learning Transferable Visual Models From Natural Language Supervision (2021)
- [125] Martino, G., Barrón-Cedeno, A., Wachsmuth, H., Petrov, R., Nakov, P.: Semeval-2020 task 11: Detection of propaganda techniques in news articles. arXiv preprint arXiv:2009.02696 (2020)
- [126] Loshchilov, I.: Decoupled weight decay regularization. arXiv preprint arXiv:1711.05101 (2017)
- [127] Li, Z., Hoiem, D.: Learning without forgetting. *IEEE Transactions on Pattern Analysis and Machine Intelligence* **40**(12), 2935–2947 (2018) <https://doi.org/10.1109/TPAMI.2017.2773081>
- [128] Lin, S., Sprague, T., Singh, A.K.: Mind reader: Reconstructing complex images from brain activities. *Advances in Neural Information Processing Systems* **35**, 29624–29636 (2022)
- [129] Ozcelik, F., VanRullen, R.: Natural scene reconstruction from fmri signals using generative latent diffusion. *Scientific Reports* **13**(1), 15666 (2023)
- [130] Chen, Z., Qing, J., Xiang, T., Yue, W.L., Zhou, J.H.: Seeing beyond the brain: Conditional diffusion model with sparse masked modeling for vision decoding. In: *Proceedings of the IEEE/CVF Conference on Computer Vision and Pattern Recognition*, pp. 22710–22720 (2023)